Journal of the European Ceramic Society 15 (1995) 959–965
© 1995 Elsevier Science Limited
Printed in Great Britain. All rights reserved
0955-2219/95/$9.50

0955-2219(95)00065-8

Processing of Nano-Y–TZP/Al_2O_3 Composites. I: Preparation and Characterization of Nano-Y–TZP/Al_2O_3 Composite Powders

J. L. Shi, B. S. Li, M. L. Ruan & T. S. Yen

Shanghai Institute of Ceramics, Chinese Academy of Sciences, 1295 Ding-Xi Road, Shanghai, 200050, P.R. China

(Received 31 August 1994; revised 9 March 1995; accepted 20 March 1995)

Abstract

Nano-sized and well dispersed Y–TZP/alumina (Y–TZP-rich) composite powders have been prepared via a chemical method. It has been found that alumina exists metastably in the Y–TZP lattice in the composite powders at relatively low temperatures before the crystallization of α-alumina from the composites started at around 1200°C. Alumina in the composite powders impedes the crystallite growth of Y–TZP and increases the specific surface area of the composite powders. This effect is discussed and attributed to the lattice distortion of Y–TZP by alumina.

1 Introduction

Ceramic composites are of great interest to ceramists because they exhibit better performance than their individual component materials, for example, fibre and whisker-reinforced ceramics.[1,2] However, as it is well known, fibers and whiskers are expensive and sometimes toxic, and these composites are technically difficult to densify because of the impedance of the second phase to the densification of the matrix phases. Generally hot-pressing or hot isostatic-pressing techniques are used, and thus the cost of fabricating these composites are relatively high. Another kind of ceramic composite, the particle/particle composites are, however, relatively easy technically to fabricate and are thus cheap.

Zirconia (or Y–TZP, yttria stabilized tetragonal zirconia polycrystals)/alumina composite is one of the most investigated ceramic composites, from their phase stability to mechanical properties.[3–10] Zirconia is usually used as the reinforcement agent in alumina.[6–7] However, for Y–TZP matrix/alumina particles composites, the mechanical properties of the composites were also found to be significantly better than single phase Y–TZP material.[8–10] The sinterability of the composites depends on the particle properties. Defining R as the size ratio of the second phase to the matrix phase, (the matrix Y–TZP phase assumed to be easy to densify), the densification of the matrix is greatly impeded when $R \approx 100$,[11–13] which results from the inner back stress around the second particles opposite to the sintering stress; if $R \approx 10$, the back stress is believed to be smaller, and the composite can be pressurelessly sintered, but higher sintering temperatures are needed because of the bimodal pore size distributions in the composites.[14] Supposing that the R value decreases further to about 1 — the two factors affecting the densification: back stress and the duplex pore size distribution can be minimized or even cleared out, so the sinterability of the composites will not be affected significantly.

Composite powders of $R = 1$ can be prepared by chemical methods. Rejandran *et al.*[15] Exter[16] and others[17] have prepared the composite powders using the coprecipitation method resulting in very large specific areas. However, these composite powders were still difficult to fully densify via pressureless sintering. We believe that the problem is due to the agglomeration effect of the composite powders, and hardly any individual particles in the powder can be identified.

To obtain good powder properties, the composite powders were prepared using the coprecipitation method and care was taken with the coprecipitation and washing processes. In this paper, the preparation and characterization of the Y–TZP/alumina composite powders will be reported; the compaction and sintering behavior will be presented in the next paper.

2 Experimental Procedure

2.1 Powder preparation

The Y–TZP/alumina composite powders were prepared using a common coprecipitation method, which is described as follows: (1) Preparation of the solutions of Zr^{4+}, Y^{3+} and Al^{3+} from zirconium oxychloride (chemical grade), respectively, with their concentrations determined by chemical methods. (2) Preparation of the mutual solutions with designated ratios of Zr:Y:Al. (3) Putting the solution into a 12 vol% concentrated ammonia solution and yielding the coprecipitates. The pH value of the solutions after coprecipitation was maintained at around 8–9. (4) Washing the coprecipitates with distilled water until the concentration of Cl^- in filtrates were less than 10 ppm. (5) Washing the cake further with ethanol for approximately six times until the water content in the filtrates measures less than 6 vol%. (6) Drying the coprecipitates overnight at 80°C, followed by calcination in air at different temperatures from 420 to 1350°C for 120 min. After the above steps, the composite oxide powders were obtained.

2.2 Powder characterization

The composite powders were characterized as follows:

2.2.1 Specific surface area

The specific surface area of the composite powders was measured with multi-point nitrogen adsorption BET method (Micromeritics, 220/50000/OX). The particle sizes of the composite powders were calculated by assuming the spherical shape of the powder particles.

2.2.2 Crystallite size determination

X-ray diffraction-line broadening (XRD-LB, Rigaku Denki, RAX-10) method was used for the determination of the average crystallite size of the composite powders. As a matter of fact, only the diffraction peaks of Y–TZP crystals could be obtained at less than about 1200°C, so only the crystallite sizes of Y–TZP in the composite powders were determined using its (111) diffraction peak. The half intensity breadth of the diffraction peak was calibrated by subtracting the instrumental broadening.

2.2.3 Micro-morphology observation

The crystallite size and micro-morphology of the composite powders were observed using transmission electron microscopy, (TEM, JEM-200CX, JEOL) and the composite powders were also analyzed of their components in a micro-area with energy dispersive spectroscopy (EDS) which is part of the microscope. The detailed structure of the composite crystallites were observed with a high resolution electron microscope (HREM, JEM-200CX, JEOL).

2.2.4 Phase analysis

X-ray-diffraction (Rigaku Denki, RAX-10) was used for the analysis of the phase structures. To detect the possible phases of very weak diffraction ability, very high X-ray intensity was used when the diffraction peaks of the main phase were largely out of scale.

To investigate the possible effect of alumina on the lattice distortion of Y–TZP, the (200) lattice plane distance of Y–TZP was measured using the XRD method. To prevent an instrument error, pure Y–TZP samples prepared under the same conditions as the composite powders were measured, together with other samples in every batch.

3 Results

3.1 Specific surface area as a function of alumina content

As reported by other researchers,[15,16] the specific surface area of the coprecipitated composite powders was greatly increased by the addition of alumina. This was also true for the composite powders prepared in this study, as shown in Fig. 1. Figure 2 shows the calculated particle size of

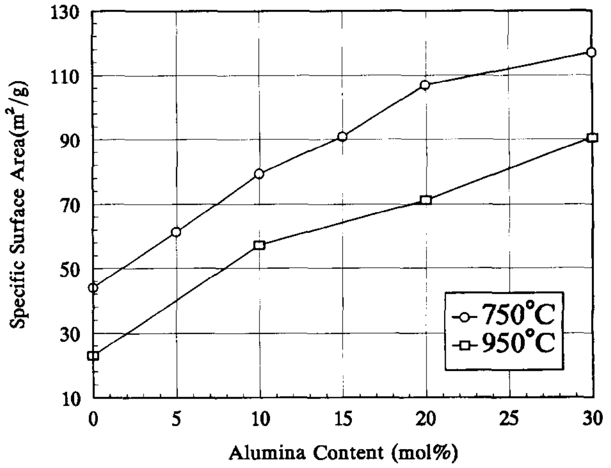

Fig. 1. Specific surface area of the composite powders as a function of alumina content, the powders were calcined at 750 and 950°C for 120 min.

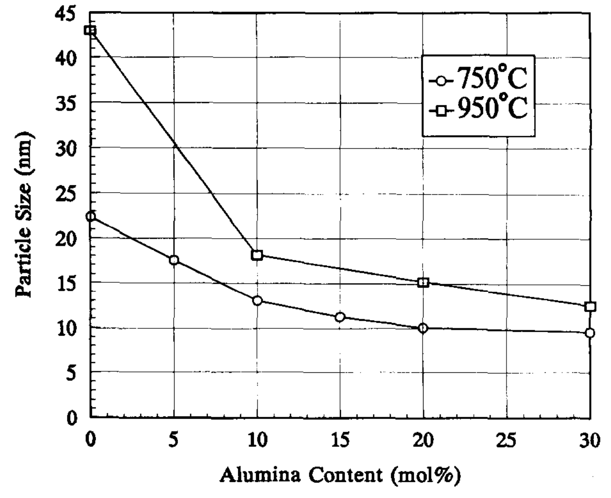

Fig. 2. Particle size calculated from the specific surface area versus alumina content.

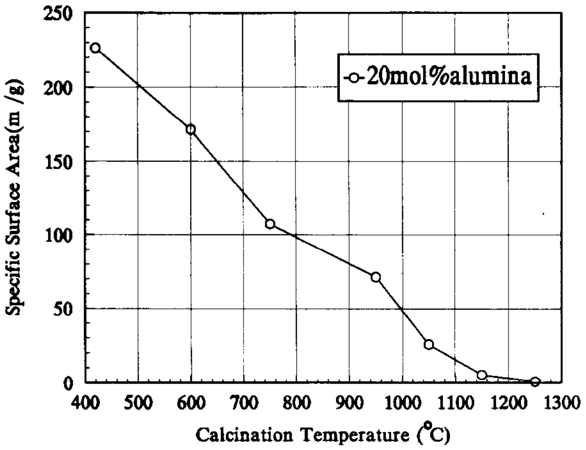

Fig. 3. Temperature dependence of the specific surface area of the Y–TZP/20 mol% alumina composite powders.

the composite powders from the specific surface area. The composite powders were very fine with extraordinarily high surface area when calcined at low temperatures such as 420 and 600°C, and decreased rapidly at elevated temperatures as illustrated in Fig. 3, which was accompanied by crystallite growth, particle coarsening and partial sintering.

3.2 Phase structure and crystallite size

The results of the XRD study for Y–TZP/20 mol% alumina composite powders (Fig. 4) shows that at less than about 1200°C, only the diffraction peaks of Y–TZP were detected but not those of alumina, even at the maximum X-ray power output of 15 kW; although γ-alumina (or other forms except for the α phase) using the same process can be detected easily under ordinary diffraction conditions.

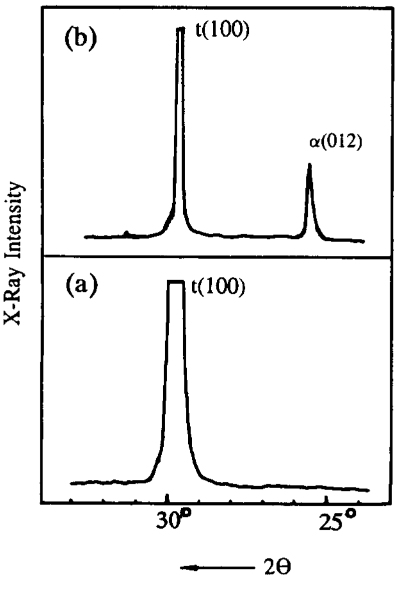

Fig. 4. XRD spectra of the Y-TZP/20 mol% alumina composite powders calcined at (a) 750°C and (b) 1250°C for 120 min.

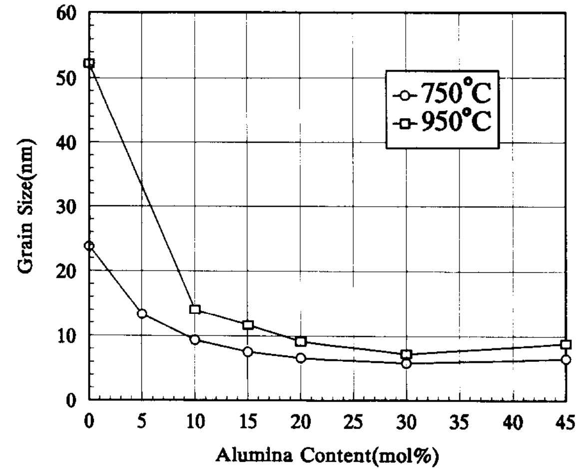

Fig. 5. Crystallite size of Y–TZP as a function of alumina content in the composite powders calcined at 750 and 950°C for 120 min.

Based on the above reason, only the crystallite sizes of Y–TZP could be determined with the method. The results are shown in Fig. 5 illustrating the effect of alumina on the crystallite size of Y–TZP, and such an effect was most important at relatively low alumina contents of 5 and 10 mol%.

3.3 Micromorphology of the composite powders

The effect of the addition of alumina on the crystallite size is shown in Fig. 6. The decrease of the crystallite size with increasing alumina content is apparent. Different from the powder micromorphology reported by Rajendran,[15] the particles were well dispersed and therefore could be identified separately from the micrographs, due to the careful control of the processes of the powder preparation. The temperature dependence of the particle size and morphology of Y–TZP/20 mol% alumina is illustrated in Fig. 7. At temperatures lower than 1250°C, there seems to be only one kind of particle present in the powders, which means no component separation can be observed under the conditions. At elevated temperatures of 1250°C or higher, the component contrasts can be seen in the micrographs, which means the component separation takes place. As shown in Fig. 7(f), the dark grains are Y–TZP and the lighter ones are alumina, as indicated by the EDS results in Fig. 8.

4 Discussion

4.1 Existing form of alumina in the composite powders

According to the phase diagrams, alumina and zirconia are insoluble with each other both at ambient and high temperatures. In the present study, this is true for the composite powders calcined at temperatures of around 1200°C when α-alumina crystallized out, as can be seen in Figs 4 and 7.

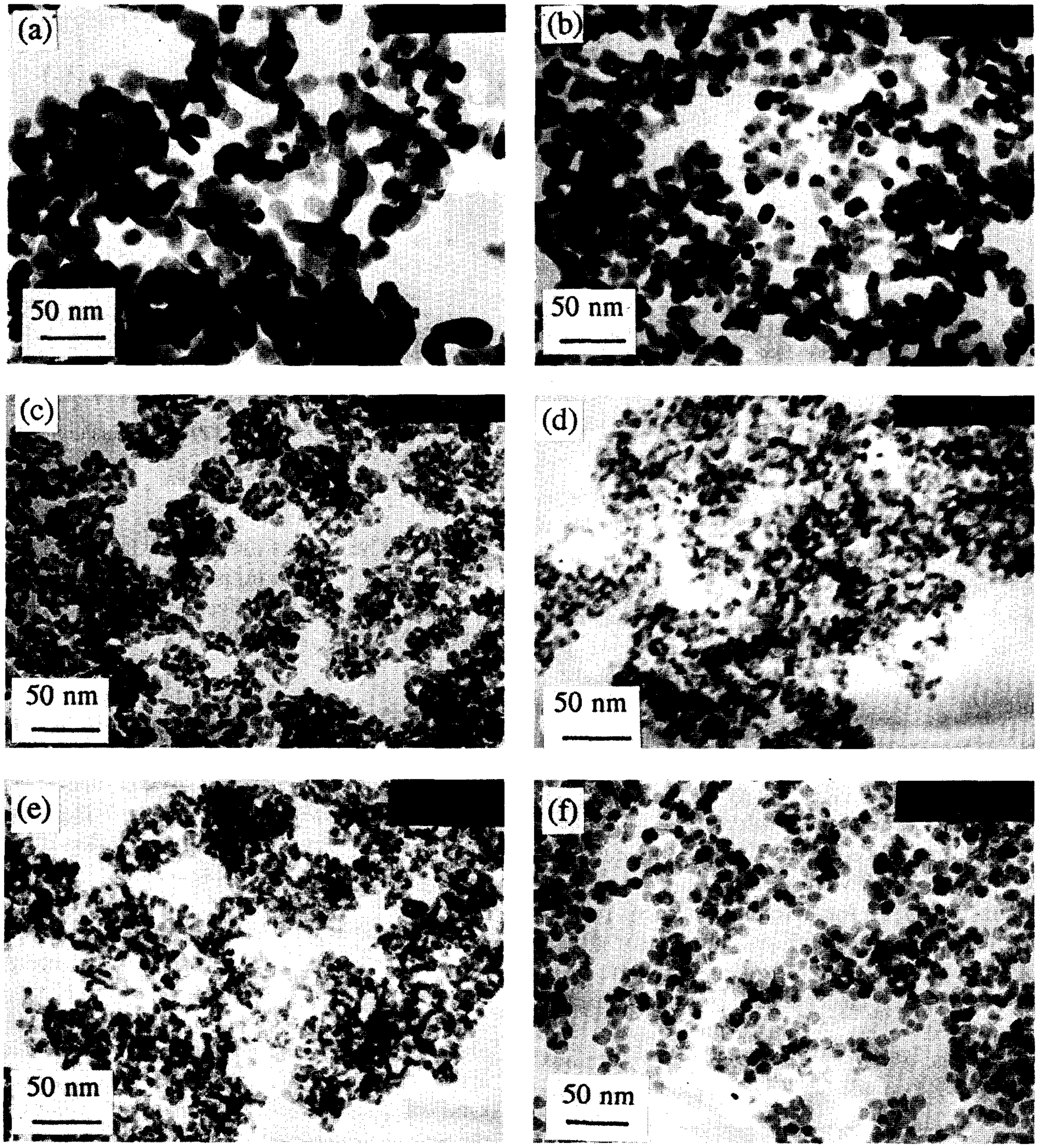

Fig. 6. TEM micrographs of the 750°C calcined composite powders containing (a) 0, (b) 5, (c) 10, (d) 20, (e) 30 and (f) 45 mol% alumina.

However, the two components (supposing yttria always dissolves in the Y–TZP lattice) were not found to exist separately from Y–TZP at lower temperatures than the crystallization point of the α phase. The detailed observation by HREM of the micromorphology of the composite powders containing 20 mol% alumina (Fig. 9) shows no alumina in the Y–TZP grains or around the grains, although alumina may be amorphous-like. However, if it existed separately from Y–TZP, there should have been a contrast between alumina and Y–TZP and between alumina and the background of carbon films which was used to support the particles. So it is believed that alumina existed in the Y–TZP lattice before the crystallization of α-alumina from the composites at around 1200°C. Direct evidence of this conclusion has been found by measuring the lattice parameters of Y–TZP, (as shown in Fig. 10), of the differences of the (200) lattice plane distances between pure Y–TZP and alumina added composite powders. Such a lattice distortion could only be attributed to the alumina existing in the Y–TZP lattice, since the lattice parameters of Y–TZP cannot be affected by alumina particles around them even in the sintered bodies.[14] Such an effect was most significant at a relatively low alumina content, which corresponded to the crystallite size decreasing effect of Y–TZP by the addition of alumina. When α-alumina crystallized out from the

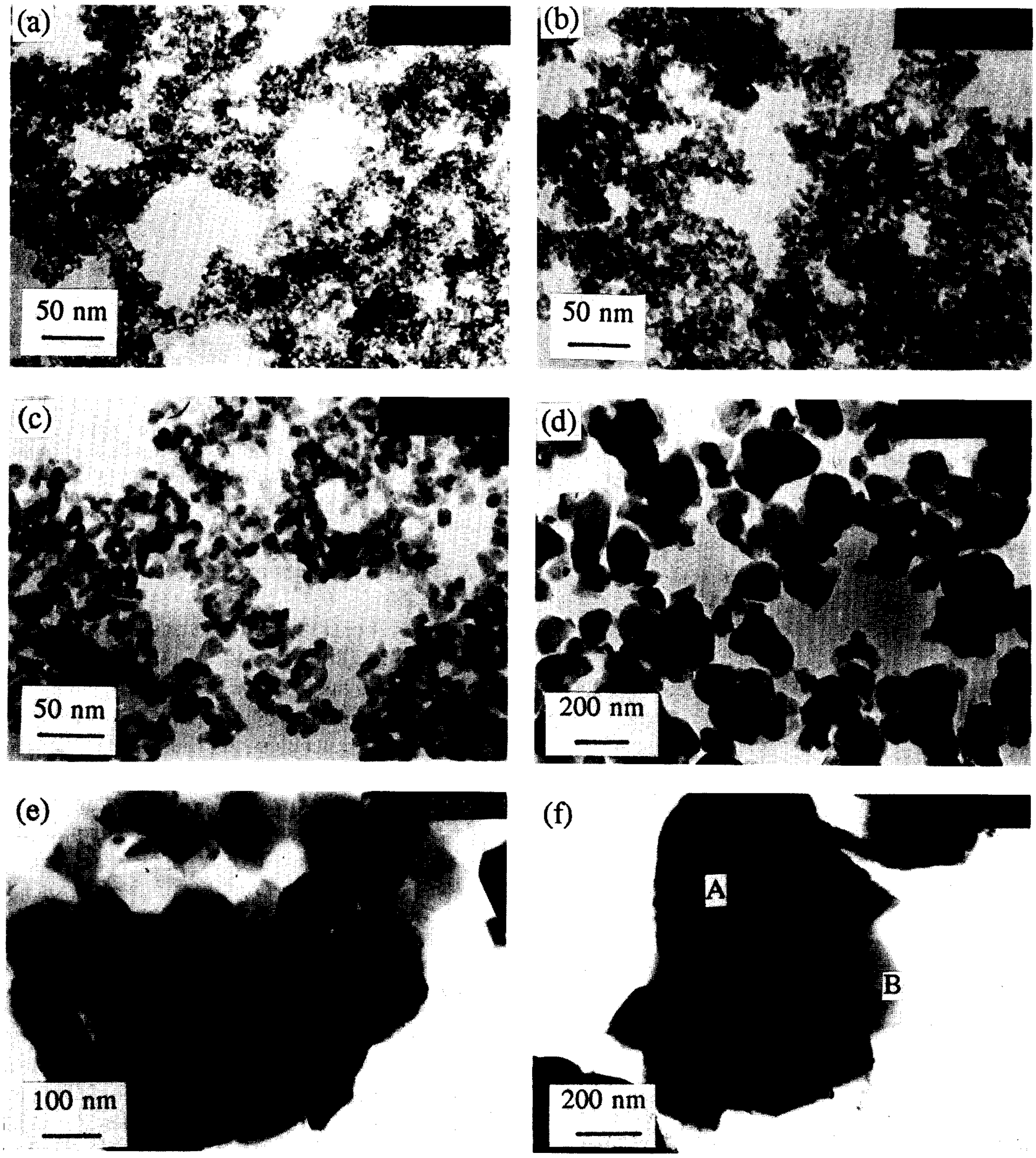

Fig. 7. TEM micrographs of the Y–TZP/20 mol% alumina composite powders calcined at (a) 420, (b) 600, (c) 950, (d) 1050, (e) 1250 and (f) 1350°C for 120 min.

composite, the difference of the lattice plane distances returned to zero, as shown in Fig. 11 for the composite powders containing 20 mol% alumina.

4.2 Crystallization process of alumina in the composite powders

Al_2O_3 presents as the γ phase (or other forms except the α phase) when decomposed from the hydroxides or other salts of aluminum at around 1200°C. These forms are amorphous-like and therefore are metastable themselves. As the phase transformation from these forms to the thermodynamically stable α phase needs a big structure rearrangement, usually a temperature range around 1200°C is required for such a transformation. For the composite powder investigated in this study, the three components were mixed homogeneously on a molecular level in their mutual solutions and such a homogeneity could be maintained in the hydroxide coprecipitates and amorphous oxides at less than about 360–400°C. Y–TZP are very easy to crystallize from its amorphous oxide at only around 400°C.[3] At this low temperature, the diffusion of alumina molecules through Y–TZP to form a separate alumina phase are difficult. This was because, firstly, the thermodynamic driving force for this process was small, as a separate alumina phase at less than 1200°C was metastable

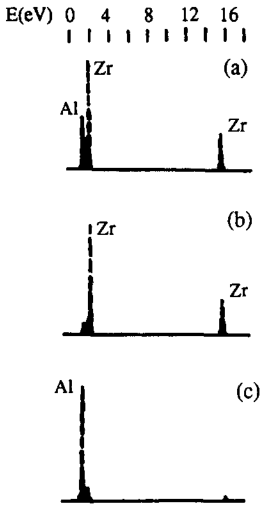

Fig. 8. EDS spectra: (a) for the sample shown in Fig. 7(c); (b) for the sample shown in Fig. 7(f) on dark area 'A' and (c) on the lighter area 'B'.

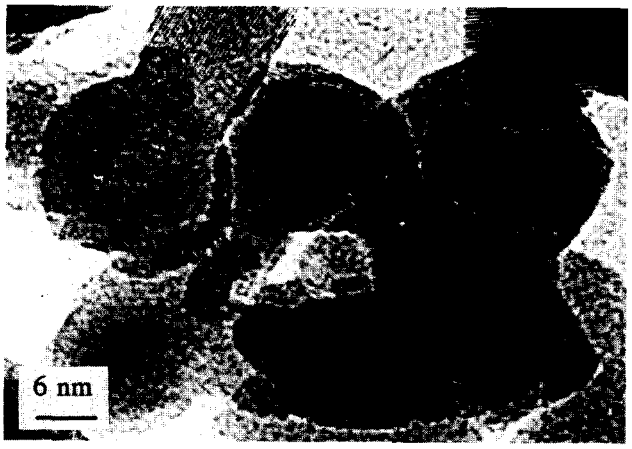

Fig. 9. HREM micrographs of Y–TZP/20 mol% alumina composite powders calcined at 950°C.

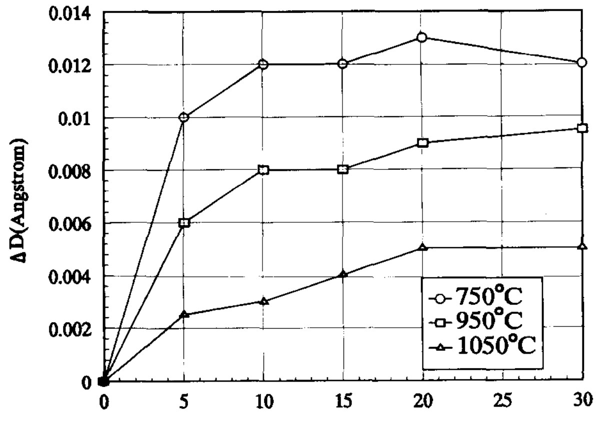

Fig. 10. Differences of the (200) lattice plane distance between pure Y–TZP and composite powders.

itself; secondly, the kinetic resistance was great because of such a low temperature and Y–TZP impedance. As temperature increases, the diffusion resistance became less and the driving force became large. At around 1200°C, thermodynamically stable α phase crystallized out and the two components became separate to one another.

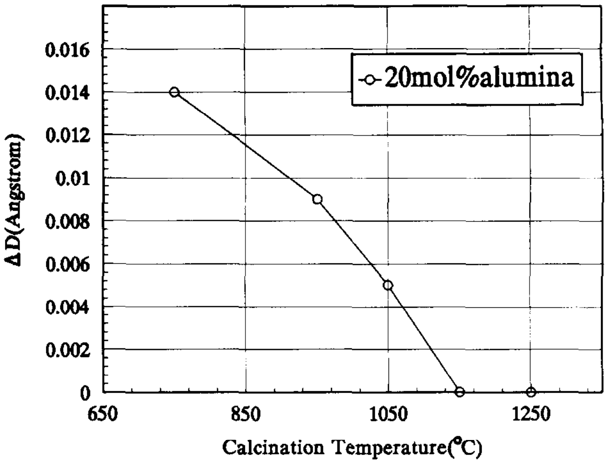

Fig. 11. Difference of the (200) lattice plane distances of Y–TZP/20 mol% alumina composite powders as a function of calcination temperature.

4.3 Influence of alumina on the crystallite growth of Y–TZP

There are possibly two reasons for the hindrance of the crystallite growth of Y–TZP by alumina: lowering the surface tension of the Y–TZP particles, or increasing the resistance for the diffusion of Y–TZP molecules. As has been argued, alumina existed homogeneously in the Y–TZP lattice before the crystallization of α-alumina from the composite powders, and the most strong effect on the crystallite growth of Y–TZP was at the relatively low alumina content of 5–10 mol%. Even so, it was still possible that some alumina components at, or near the particle surface of Y–TZP could affect the surface tension. However, this effect is believed to be limited if the homogeneous distribution of the alumina molecules in the Y–TZP lattice was true, because the amount of alumina species at the particle surface were not concentrated, which could not alter the crystallite growth behavior so much, as shown in Fig. 5. In contrast, the presence of alumina in the Y–TZP lattice caused the lattice distortion of Y–TZP, mostly at the relatively low alumina level of 5 mol%, corresponding to the dependence of crystallite size on the alumina content. The lattice distortion led by the aluminum ions would lead to the considerable additional energy fluctuations in the lattice. Such an energy fluctuation would act as the energy barrier for the diffusion of Y–TZP, so the diffusion resistance of Y–TZP species would be increased, and therefore the crystallite growth which depends on the diffusion would be impeded. So it is believed that the lattice distortion by the presence of alumina in the Y–TZP lattice is the main reason for the impedance of the crystallite growth of Y–TZP in the composite powders.

5 Conclusions

(1) Nano-sized and well dispersed Y–TZP/Al_2O_3 composite powder could be prepared by coprecipitation method with careful control of the processes.

(2) Alumina co-existed in the Y–TZP lattice at relatively low temperatures before the crystallization of the α phase from the composite powders at about 1200°C, leading to the lattice distortions of Y–TZP.

(3) The crystallite growth of Y–TZP was greatly impeded by the addition of alumina in the composite powders. The reason for this phenomenon is believed to be caused mainly by the lattice distortion led by alumina.

References

1. Maschall, D. B. & Evans, A. G., The tensile strength of uniaxially reinforced ceramic fibre composites. In *Fracture Mechanics of Ceramics, Vol. 7*, eds R. C. Bradt, A. G. Evans, D. P. H. Hasselman & F. F. Lange, Plenum, New York–London, 1986, pp. 1–16.
2. Becher, P. F., Tiegs, T. N., Ogle, J. C. & Warwick, W. H., Toughening of ceramics by whisker reinforcement, *ibid.* pp. 61–74.
3. Shi, J. L., Lin, Z. X. & Ten, T. S., Effect of alumina restraining on the stability of tetragonal zirconia composite powders. *J. Europ. Ceram. Soc.*, **9** (1992) 27–33.
4. Murase, Y., Kato, E. & Dlaiman, K., Stability of ZrO_2 phase ultrafine ZrO_2–Al_2O_3 mixtures, *J. Am. Ceram. Soc.*, **69**(2) (1986) 83.
5. Yoshimatsu, H., Kamasaki, H. & Osaka, A., Stability of tetragonal ZrO_2 phase in Al_2O_3 prepared from Zr–Al organometallic compounds, *J. Mater. Sci.*, **23** (1988) 332.
6. Masaki, T. & Shino, K., Mechanical behaviour of ZrO_2–Y_2O_3 ceramics formed by hot-isostatic pressing. In *Advances in ceramics, science and technology of zirconia III*, eds S. Somiya, N. Yamamoto & H. Hanagida, The Am. Ceram. Soc. Inc., Columbus, OH, 1988, p. 709.
7. Lange, F. F., Transformation toughening. Part 4: fabrication, fracture toughness and strength of Al_2O_3–ZrO_2 composites, *J. Mater. Sci.*, **17** (1982) 247.
8. Tsukuma, K., Takahata, T. & Shiomi, M., Strength and fracture toughness of Y–TZP, Ce–TZP, Y–TZP/Al_2O_3 and Ce–TZP/Al_2O_3. In *Advances in ceramics vol. 24, science and technology of zirconia*, eds S. Somiya, N. Yamamoto, H. Hanagida, The Am. Ceram. Soc., Columbus, OH, 1988, p. 721.
9. Shi, J. L., Li, B. S. & Yen, T. S., Mechanical properties of Al_2O_3 particle-Y–TZP matrix composite and its toughening mechanism, *J. Mater. Sci.*, **28** (1993) 4019–22.
10. Rajendran, S., Swain, M. V. & Rossell, H. J., Mechanical properties and microstructures of co-precipitation derived tetragonal Y_2O_3–ZrO_2–Al_2O_3 composites, *J. Mater. Sci.*, **23** (1988) 1805–12.
11. Tuan, W. H. & Brook, R. J., Sintering of heterogeneous composites, Part II: ZrO_2–Al_2O_3, *J. Mater. Sci.*, **24** (1989) 1953.
12. Sudre, O. & Lange, F. F., Effect of inclusions on densifications. I: microstructural development in an Al_2O_3 matrix containing a high volume fracture of ZrO_2 inclusions, *J. Am. Ceram. Soc.*, **75**(3) (1992) 519.
13. Tuan, W. H. & Brook, R. J., Sintering of heterogeneous ceramic composites, Part I: Al_2O_3–Al_2O_3, *J. Mater. Sci.*, **24** (1989) 1062.
14. Shi, J. L. & Yen, T. S., Densification and microstructure development of alumina/Y–TZP composite powder (Y–TZP-rich) compacts, *J. Euro. Ceram. Soc.*, in press.
15. Rejandran, S., Rossell, H. J. & Sanders, J. V., Preparation and characterization of precursors powders for yttria-doped tetragonal zirconia polycrystals (Y–TZP) and Y–TZP–Al_2O_3 composites, *J. Mater. Sci.*, **24** (1989) 1195–202.
16. der Exter, P., Winnubst, A. J. A. & Burggraaf, A. J., The preparation and characterization of Y–TZP/20 vol% Al_2O_3, *J. Euro. Ceram. Soc.*, **11** (1993) 497.
17. Navarro, L .M., Recio, P., Jurado, J. R. & Duran, P., Development of high density Y_2O_3–ZrO_2–Al_2O_3 composites as solid electrolyte for SOFC. In Proceedings of Third Euro-Ceramics Vol. 2, ed. P. Duran & J. F. Fernandez, Faenza Editrice Iberuca S. L., 1993, p. 281–6.